

## String Breaking as a Mixing Phenomenon in the SU(2) Higgs Model



Francesco Knechtli <sup>a †</sup> and Rainer Sommer <sup>b ‡</sup>

<sup>a</sup> Physics Department, University of Colorado, Boulder, CO 80309 USA

<sup>b</sup> DESY, Platanenallee 6, D-15738 Zeuthen, Germany

### Abstract

We study the potential of a static quark anti-quark pair in the confinement “phase” of the SU(2) Higgs model. Around separation  $r_b$ , the confining string of the gauge field breaks by formation of a dynamical pair of light quarks. The ground state and first excited state static potentials are determined by a variational technique from a matrix correlation in which suitably smeared gauge and Higgs fields enter. Our results at  $\beta = 2.4$  clearly show string breaking ( $r_b \approx 1.9r_0$ ). The investigation of properly defined overlaps confirms the interpretation of string breaking as a level crossing phenomenon between string-type and meson-type states. We study the scaling properties of the static potentials along a line of constant physics, varying the lattice spacing by a factor of 2. Our results show compatibility with scaling within tiny errors.

COLO-HEP-444  
DESY 00-078  
May 2000

<sup>†</sup> e-mail: knechtli@pizero.colorado.edu

<sup>‡</sup> e-mail: sommer@ifh.de

## 1 Introduction

The potential of a static quark<sup>1</sup> anti-quark pair in a Yang-Mills gauge theory has been computed by Monte Carlo simulations on the lattice. The observable from which the static potential is extracted is the Wilson loop. The results for gauge group SU(2) [1,2] and SU(3) [3,4], close to the continuum limit, show a linearly rising confinement potential at large separations of the static charges. When the Yang-Mills gauge theories are coupled to matter fields in the fundamental representation of the gauge group, the static potential is expected to flatten at large distances: the ground state of the system is better interpreted in terms of two weakly interacting static-light mesons which are bound states of a static and a dynamical quark. The dynamical quarks are pair-created in the strong gauge field binding the static quarks. This phenomenon is called *string breaking* or *screening* of the static charges. The name “string” refers to the gauge field configuration which confines the static quarks and leads to the linear confinement in pure gauge theories.

In recent attempts in QCD with two flavors of dynamical quarks [5,6,7,8,9,10,11], the flattening in the static potential determined from the Wilson loops was not visible. The string breaking distance  $r_b$  around which the static potential should start flattening off, could nevertheless be estimated in the quenched approximation of QCD to be [12,13]

$$r_b \approx 2.7r_0, \quad (1)$$

where  $r_0 \approx 0.5 \text{ fm}$  is a scale conveniently defined from the force,  $F(r)$ , between static quarks[2]:

$$F(r_0)r_0^2 = 1.65r_0, \quad (2)$$

The QCD results so far show a linear rise of the static potential for distances beyond  $r_b$ . It has been commonly argued that the problem is the poor overlap of the Wilson loops with the ground state of the system. The investigation of the static potential in models other than QCD is therefore relevant in order to understand its origin and identify the reason for the failure of the method used to extract it in full QCD.

First studies of string breaking were performed with a hopping-parameter expansion in SU(2) gauge theory with Wilson fermions [14]. In the Schwinger model (QED<sub>2</sub>), the exact solution for the static potential can be given in the limit of zero fermion mass [15]:  $V(r) = (e\sqrt{\pi}/2)\{1 - \exp(-er/\sqrt{\pi})\}$ , where  $e$  is the charge of the static sources. String breaking was established by numerical simulation in the Schwinger model [16,17]. Numerical evidence of the screening of the static potential was also found in the U(1) Higgs model (scalar QED) in two dimensions [18]. The flattening of the static potential at large distances is also expected in the confinement “phase” of the SU(2) Higgs model. Indeed, early simulations yielded some qualitative evidence for string breaking [19,20].

---

<sup>1</sup> A static quark (anti-quark) is an external source in the (complex conjugate of the) fundamental representation of the gauge group.

String breaking can also be studied in Yang-Mills theories using static sources in the adjoint representation of the gauge group. The gauge field itself is responsible for the screening of the sources and the formation of hadrons called “gluelumps”. An important numerical investigation concerning this screening has been carried out by C. Michael in [21], where it has been noted that string breaking can be a *mixing* phenomenon. The static potential is extracted from a matrix correlation in which two types of states enter, the adjoint string and the “two-gluelump”. However, due to large errors, no clear evidence for string breaking could be given. The first numerical evidence for string breaking in non-Abelian gauge theories with dynamical matter fields was given using the mixing method in the four-dimensional [22] and three-dimensional [23] SU(2) Higgs model by the computation of the potential between static quarks. Most recently, the extraction of the static adjoint potential in the three-dimensional [24,25] and four-dimensional [26] SU(2) Yang-Mills theory shows also evidence for string breaking.

In full QCD, string breaking has been seen at finite temperature [27], where the static potential can be extracted from Polyakov loop correlators. A recent investigation in zero-temperature QCD with two flavors of dynamical quarks [28] gives some indication that string breaking can be observed in the potential determined from a matrix correlation containing string-type and meson-type states. The main problems are the computational costs of the light quark propagators entering the matrix correlation: the maximal variance reduction method of [29] has been applied in [28].

In this article, we present results for the spectrum of static-light mesons and for the static potential in the confinement “phase” of the SU(2) Higgs model. The method of computation of the static potential is the same as in our first work [22] but it is explained here in much more detail. In Sect. 2, we present a detailed investigation of the spectrum of the static-light mesons. This is relevant not only for determining the asymptotic value of the static potential, but also for finding a suitable smearing procedure for the Higgs field to be used in the computation of the static potential. In Sect. 3, we show our results for the ground state and the first excited static potential obtained at  $\beta = 2.4$ , with a spatial resolution two times better than at  $\beta = 2.2$  used in [22].

In order to study the interpretation of string breaking as a mixing phenomenon [30] we first properly define overlaps of the string and two-meson states with the ground and first excited energy eigenstates. Their dependence on the distance  $r$  then establishes string breaking as a level crossing phenomenon. In Sect. 4, we study the scaling of the static potentials by comparing the results at  $\beta = 2.4$  with  $\beta = 2.2$  on a line of constant physics [31]. The dependence of the static potentials on the value of the Higgs quartic self-coupling is also investigated.

## 2 The spectrum of the static-light mesons

The investigation of the spectrum of static-light mesons is an important study to be done before the extraction of the static potential. The system composed by a static quark

anti-quark pair is expected to be described at large separation of the static sources by two weakly interacting static-light mesons, which are bound states of a static quark and the dynamical matter field. Denoting by  $\mu$  the mass of the lowest meson state, the static potential  $V_0(r)$  is expected to approach the value

$$\lim_{r \rightarrow \infty} V_0(r) = 2\mu. \quad (3)$$

Therefore, the mass  $\mu$  basically determines the string breaking distance  $r_b$  around which the potential starts flattening out.

The extraction of the static-light meson spectrum is representative for the variational method that we employ also for the extraction of the static potential. We constructed a large basis of operators that create one-meson “states” when applied to the vacuum. The variational approach chooses the best linear combinations of these “states” which approximate the energy eigenstates. Through the determination of the meson spectrum we can therefore gain information about a suitable way of constructing the meson-type states. Then, we use this information in Sect. 3 to construct a basis of states for the determination of the static potentials.

## 2.1 The matrix correlation

In [32], an Hamiltonian formalism for the SU(2) Higgs model is constructed. Along the lines of [33], a *transfer matrix operator* is defined and its strict positivity for  $\kappa > 0$  and  $\lambda > 0$  is proved<sup>2</sup>. This property is equivalent to the reality of the energy spectrum in any sector of the Hilbert space. Different *charge sectors* of the Hilbert space are defined by the transformation property of the states under gauge transformation. Through Gauss’ law, this gauge transformation property is related to the presence of static charges in some irreducible representation of the gauge group.

The static-light meson states belong to the charge sector with one static charge in the fundamental representation of the gauge group localised at a certain space position  $\vec{x}$ . The meson states  $|i\rangle$ , ( $i = 1, 2, 3, \dots$ ), are described by (composite) fields  $O_i^M(x)$ , which are constructed with field variables taken at equal time  $x_0$  and transform under a gauge transformation  $\{\Lambda(x) \in \text{SU}(2)\}$  according to

$$[O_i^{M,\Lambda}(x)]_a = \Lambda_{aa'}^\dagger(x)[O_i^M(x)]_{a'}, \quad (4)$$

where  $a, a' = 1, 2$  are color indices. The obvious choice is to take  $O^M(x)$  to be the Higgs field  $\Phi(x)$ . We are also going to consider non-local linear combinations which take into account contributions from Higgs fields at neighboring sites (smeared fields) and more

---

<sup>2</sup> One can show that the partition function of the SU(2) Higgs model satisfies the property  $Z(\beta, \kappa, \lambda) = Z(\beta, -\kappa, \lambda)$ . There is a mapping of the observables such that the expectation values at positive  $\kappa$  are reproduced by expectation values at negative  $\kappa$ . This motivates the restriction of the parameter region to the values  $\kappa > 0$ . For  $\lambda = 0$ , strict positivity of the transfer matrix holds for  $0 < \kappa < 1/6$ .

general composite fields, with the intent to model the true wave function of the meson. From the basis of meson-type fields  $O_i^M(x)$  a matrix correlation

$$C_{ij}^M(t) = \langle [O_j^M(x + t\hat{0})^*]_a U(x, x + t\hat{0})_{ab}^\dagger [O_i^M(x)]_b \rangle. \quad (5)$$

is constructed representing the transition amplitude over a time interval  $t$  from the meson state  $i$  to the meson state  $j$ . The static charge is represented by a straight time-like Wilson line  $U(x, x + t\hat{0})^\dagger$  connecting  $x$  with  $x + t\hat{0}$ . With the help of the reconstruction theorem proved in [32], it is possible to show that in the limit of an infinite physical time extension  $T$  of the lattice<sup>3</sup> the correlation matrix eq. (5) can be written like

$$C_{ij}^M(t) = \sum_{\alpha} \langle j|\alpha\rangle \langle \alpha|i\rangle e^{-tW_{\alpha}}, \quad (6)$$

where  $|\alpha\rangle$ , ( $\alpha = 0, 1, 2, \dots$ ) are the orthonormal meson energy-eigenstates with energies<sup>4</sup>  $W_{\alpha}$ ,  $W_{\alpha} < W_{\alpha+1}$ . The matrix correlation eq. (5) can be measured in a Monte Carlo simulation: now, we describe the variational method for extracting the meson energy spectrum from it.

## 2.2 Variational method

For matrices of the type in eq. (6) a general lemma for the extraction of the energies  $W_{\alpha}$  has been proved in [34]. In this reference, a variational method is proposed, which is superior to a straightforward application of the lemma. It consists in solving the generalised eigenvalue problem:

$$\sum_j C_{ij}(t) v_{\alpha,j}(t, t_0) = \lambda_{\alpha}(t, t_0) \sum_j C_{ij}(t_0) v_{\alpha,j}(t, t_0), \quad \lambda_{\alpha} > \lambda_{\alpha+1}, \quad (7)$$

where  $t_0$  is fixed and small (in practice we use  $t_0 = 0$ ). The generalised eigenvalues  $\lambda_{\alpha}(t, t_0)$  are computed as the eigenvalues of  $\bar{C} = C(t_0)^{-1/2} C(t) C(t_0)^{-1/2}$  and the vectors

$$\bar{v}_{\alpha,i} = \sum_j [C(t_0)^{1/2}]_{ij} v_{\alpha,j}(t, t_0) \quad \text{with} \quad \sum_i \bar{v}_{\alpha,i} \bar{v}_{\alpha',i} = \delta_{\alpha\alpha'} \quad (8)$$

are the orthonormal eigenvectors of  $\bar{C}$ . The positivity of the transfer matrix ensures that  $C(t)$  is positive definite for all  $t$ . In [34] it is proven that the energies  $W_{\alpha}$  are given by the expressions

$$aW_{\alpha} = \ln(\lambda_{\alpha}(t - a, t_0) / \lambda_{\alpha}(t, t_0)) + O\left(e^{-t\Delta W_{\alpha}}\right), \quad (9)$$

where  $\Delta W_{\alpha} = \min_{\beta \neq \alpha} |W_{\alpha} - W_{\beta}|$ . It is expected that, for a good basis of states, the coefficients of the higher exponential corrections in eq. (9) are suppressed so that the

<sup>3</sup> In practice, the limit  $T \rightarrow \infty$  is reached when  $Tm_H \gg 1$ , where  $m_H$  is the Higgs mass defined as the mass gap in the zero charge (gauge invariant) sector of the Hilbert space.

<sup>4</sup> We normalise the vacuum energy to be 0.

energies can be read off at moderately large values of  $t$  from the right-hand side of eq. (9).

The variational method eq. (7) and eq. (9) is our standard method for extracting the energy spectrum. What we have stated here about this method is valid for *any* charge sector of the Hilbert space. One has to start from a basis  $|i\rangle$  of states belonging to that charge sector. The matrix correlation  $C_{ij}(t)$  corresponds to matrix elements  $\langle j|\mathbb{T}^n|i\rangle$ ,  $n \equiv t/a$ , of powers of the transfer matrix operator  $\mathbb{T}$  appropriate for the charge sector. In [32], this correspondence is derived in detail for the sector with a static quark anti-quark pair: the energy spectrum are the static potential and its excitations.

### 2.3 Smearred Higgs fields

We studied different bases of meson-type fields  $O_i^M(x)$  by measuring in Monte Carlo simulations the matrix correlation function  $C_{ij}(t)$  defined in eq. (5) and computing from it the energy spectrum of the static-light mesons using the variational method described in Sect. 2.2. Our aim was to find the best field basis for describing the ground state of the static-light mesons. For these studies we simulated the SU(2) Higgs model on a  $20^4$  lattice with parameters  $\beta = 2.2$ ,  $\kappa = 0.274$  and  $\lambda = 0.5$ . This parameter point is in the confinement “phase” of the model and is the point that we used in our first work [22]. The measurement of the matrix correlation is improved by the use of the one-link integral method [35].

We first studied a basis containing the fundamental Higgs field  $\Phi(x)$  and smeared Higgs fields obtained by iterating the application of a smearing operator  $S_1$  to the Higgs field. The smearing operator  $S_1$  is defined as

$$S_1 \Phi(x) = \Phi(x) + \sum_{\substack{|x-y|=a \\ x_0=y_0}} U(x,y)\Phi(y), \quad (10)$$

where  $U(x,y)$  is the link connecting  $y$  with  $x$ . Iterating the smearing operator  $S_1$  we obtain smeared Higgs fields  $\Phi_1^{(m)}(x) = S_1^m \Phi(x)$ , ( $m = 0, 1, 2, \dots$ ), with different smearing levels  $m$  ( $m = 0$  corresponds to the fundamental Higgs field in the Lagrangian). We measured a matrix correlation function with a basis of smeared Higgs fields corresponding to smearing levels 0,1 and 2 of  $S_1$ . The result for the ground state extracted according to eq. (9) is shown in Fig. 1 (triangles). We were not able to reach a plateau for the ratio  $\ln(\lambda_\alpha(t-a)/\lambda_\alpha(t))$  within the range of  $t$  considered (up to 8 in lattice unit).

Then, we investigated a larger basis of meson-type fields, defining in particular a smearing operator  $S_2$  as

$$S_2 \Phi(x) = \mathcal{P}\{\mathcal{P}\Phi(x) + \mathcal{P} \sum_{\substack{|x-y|=\sqrt{2}a \\ x_0=y_0}} \bar{U}(x,y)\Phi(y) + \mathcal{P} \sum_{\substack{|x-y|=\sqrt{3}a \\ x_0=y_0}} \bar{U}(x,y)\Phi(y)\}, \quad (11)$$

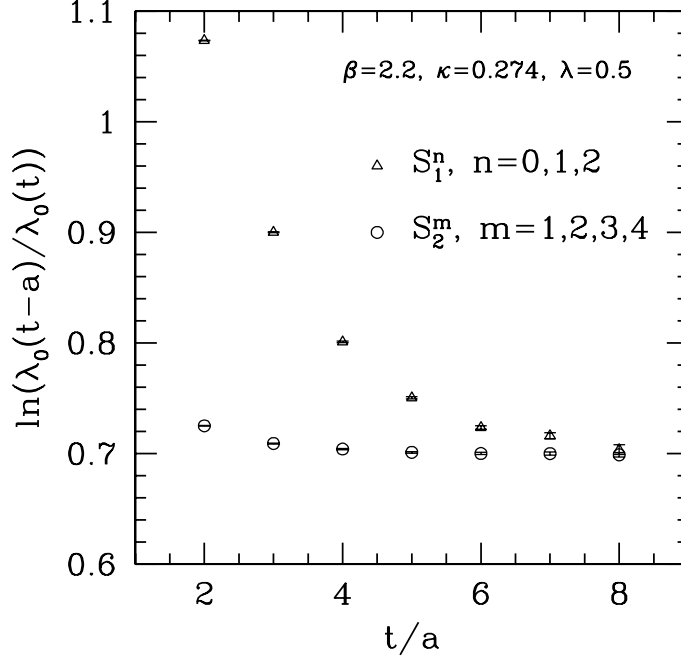


**Figure 1:** Here, we compare the extraction of the mass  $\mu$  of a static-light meson using different smearing operators defined in eq. (10) and eq. (11). The smearing levels used are indicated by  $n$  and  $m$ .

where  $\mathcal{P}\Phi = \Phi/\sqrt{\Phi^\dagger\Phi}$  and  $\bar{U}(x, y)$  represents the average over the shortest link connections between  $y$  and  $x$ . Through iteration of  $S_2$  we obtain the smeared Higgs fields  $\Phi_2^{(m)}(x) = S_2^m \Phi(x)$ , ( $m = 0, 1, 2, \dots$ ). We considered the following basis of meson-type fields  $O_i^M(x)$ ,  $i = 1, 2, \dots, 11$ :

$$O_1^M(x) = \mathcal{P}\Phi(x), \quad (12)$$

$$O_2^M(x) = \mathcal{P} \sum_{\substack{|x-y|=a \\ x_0=y_0}} U(x, y)\Phi(y), \quad (13)$$

$$O_3^M(x) = \mathcal{P} \sum_{\substack{|x-y|=\sqrt{2}a \\ x_0=y_0}} \bar{U}(x, y)\Phi(y), \quad (14)$$

$$O_4^M(x) = \mathcal{P} \sum_{\substack{|x-y|=\sqrt{3}a \\ x_0=y_0}} \bar{U}(x, y)\Phi(y), \quad (15)$$

$$O_i^M(x) = \Phi_2^{(i-4)}(x), \quad i = 5, 6, 7, 8, \quad (16)$$

$$O_9^M(x) = \Phi(x) \times \frac{1}{6} \sum_{k=1}^3 \{\Phi^\dagger(x - a\hat{k})U(x - a\hat{k}, k)\Phi(x) +$$

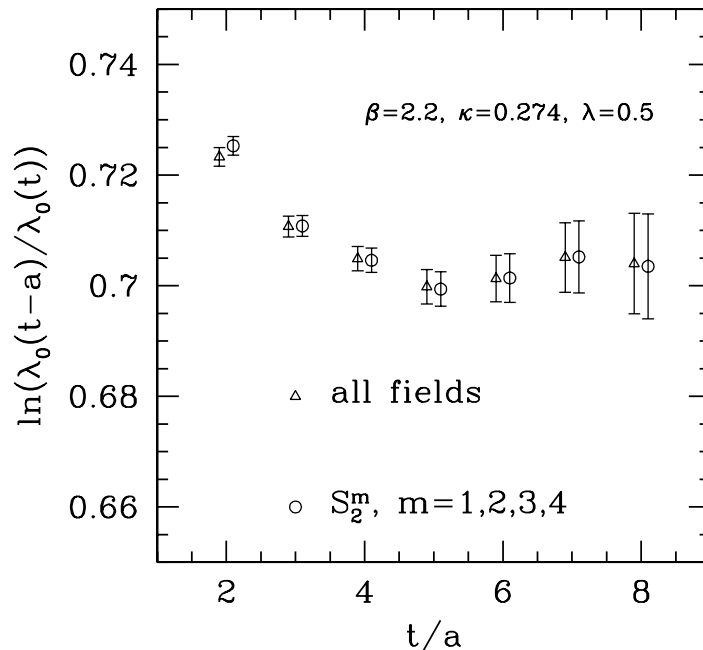


**Figure 2:** Here, we compare the extraction of the mass  $\mu$  of a static-light meson using all the fields eq. (12)–eq. (19) and only the smeared Higgs fields corresponding to smearing levels 1,2,3,4 of the smearing operator  $S_2$  defined in eq. (11).

$$\Phi^\dagger(x)U(x,k)\Phi(x+a\hat{k}), \quad (17)$$

$$O_{10}^M(x) = \Phi(x) \times \frac{1}{12} \sum_{1 \leq k < l \leq 3} \{P_{kl}(x) + P_{kl}(x - a\hat{k}) + P_{kl}(x - a\hat{k} - a\hat{l}) + P_{kl}(x - a\hat{l})\}, \quad (18)$$

$$O_{11}^M(x) = \Phi(x) \times (\Phi^\dagger(x)\Phi(x)), \quad (19)$$

where in eq. (18)  $P_{kl}(x) = U(x,k)U(x+a\hat{k},l)U^\dagger(x+a\hat{l},k)U^\dagger(x,l)$  and we use the same notation conventions as in [22]. In Fig. 2, the result for the extraction of the mass of a static-light meson using the fields  $O_i^M(x)$ ,  $i = 1, \dots, 11$  is shown (triangles). Note the enlarged scale on the y-axis as compared to Fig. 1. We obtain a nice plateau already at moderately large values of  $t$ . The situation remains practically unchanged (also the statistical errors) if we remove from the basis all fields except the smeared fields obtained by iterations of the smearing operator  $S_2$ . This means that this smearing procedure contains all relevant features for describing the ground state which could be obtained by using the larger basis.

When the generalised eigenvalue problem eq. (7) is solved, the optimal linear combination of the basis fields  $O_i^M(x)$  describing the ground state can be expressed in terms



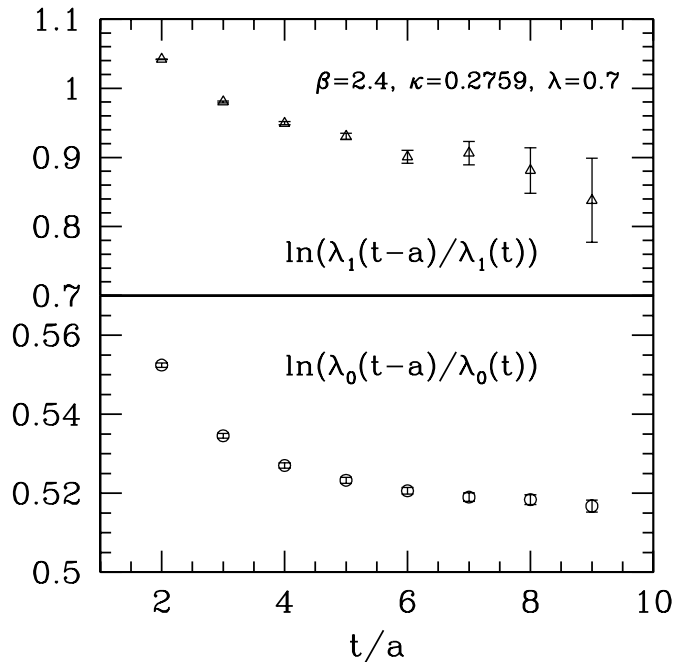


**Figure 3:** Here, we show the extraction of the mass of the ground and first excited meson state at  $\beta = 2.4$ . The basis of meson-type fields was obtained using the smearing procedure  $S_2$  eq. (11) with smearing levels  $m = 1, 3, 5, 7, 10, 15$ . The simulation was performed on a  $32^4$  lattice and the statistics is of 800 measurements.

of the components of the vector  $v_0$  as  $\sum_i v_{0,i} O_i^M(x)$ . Therefore, we call  $v_0$  the ground state wave function. An interesting fact we can learn from  $v_0$ , is that the field  $O_2^M$ , with nearest neighbor contributions, has a very small coefficient  $v_{0,2}$ . This explains our original difficulties in extracting the meson ground state. In Fig. 1, a direct comparison of the smearing operators  $S_1$  and  $S_2$  shows clearly that the contributions from the excited states are much more suppressed when we use  $S_2$  (circles).

#### 2.4 The meson spectrum at $\beta = 2.4$

In Fig. 3, we show the results for the static-light meson spectrum that we obtained for the parameters  $\beta = 2.4$ ,  $\kappa = 0.2759$ ,  $\lambda = 0.7$  (in the confinement “phase”) on a  $32^4$  lattice. More details about this simulation will be given in Sect. 3. For the measurement of the matrix correlation function we used a basis with the six fields

$$\Phi_2^{(m)}(x), \quad m = 1, 3, 5, 7, 10, 15, \quad (20)$$

obtained by iterating the smearing procedure  $S_2$  in eq. (11). As we will see in Sect. 3, the lattice spacing at  $\beta = 2.4$  is reduced by almost a factor two with respect to the

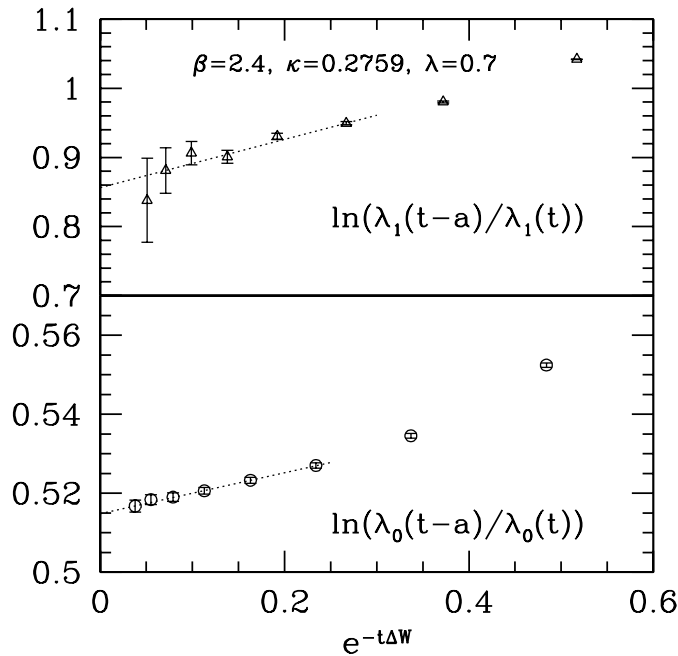


**Figure 4:** Here, we show the same data as in Fig. 3 but plotted against the correction term  $\exp(-t\Delta W)$  in eq. (9). We use  $\Delta W = \mu^* - \mu$  for the ground state and  $\Delta W = \mu^{**} - \mu^*$  for the first excited state, see (21).

lattice spacing at  $\beta = 2.2$ . Therefore, at  $\beta = 2.4$  smeared fields with high smearing levels  $m$  are expected to play a more important role than at  $\beta = 2.2$ . This expectation is confirmed by the simulation. In order to determine with confidence the static-light meson masses, we plot in Fig. 4 the logarithmic ratios on the right-hand side of eq. (9) as functions of the correction terms  $\exp(-t\Delta W)$ . This enables us to choose the best time  $t$  for reading off the masses from the logarithmic ratios and to estimate the systematic errors associated with this choice. For the mass of the ground state, we must take the largest value  $t/a = 9$ . For the mass of the first excited state, we can take  $t/a = 8$ . In both cases, the systematic errors<sup>5</sup> are of the same magnitude as the statistical errors. However, these errors are small. The results for the meson spectrum are<sup>6</sup>

$$a\mu = 0.517(2), \quad a\mu^* = 0.88(3), \quad a\mu^{**} = 1.21(9). \quad (21)$$

We note that the convergence of the right-hand side of eq. (9) is not so “critical” in the case of the static potentials considered in Sect. 3.

<sup>5</sup> The systematic errors for the masses are estimated from the difference between the mass read off at the chosen value of  $t$  and the crossing point of the dotted lines in Fig. 4 with the y-axis ( $t = \infty$ ).

<sup>6</sup> We use the notation  $\mu, \mu^*$  and  $\mu^{**}$  for  $W_0, W_1$  and  $W_2$  respectively.

### 3 String breaking and mixing

As mentioned in the introduction, the basic point concerning the determination of the static potential has been first noted by C. Michael [21] in a study of the SU(2) static adjoint potential. The energy-eigenstates of the system composed of a static quark anti-quark pair and of light dynamical matter fields are well described by a superposition of string-type and meson-type states. Using a suitable basis of such states a matrix correlation can be constructed from which the static potential and its excitations are extracted for arbitrary separations of the static quarks.

#### 3.1 The matrix correlation

The static potentials are defined as the energy levels in the charge sector of the Hilbert space with a static quark at space position  $\vec{x}$  and a static anti-quark at space position  $\vec{x}_r = \vec{x} + r\hat{k}$ . States living in this charge sector are described by fields  $O_{ab}(x, x_r)$  with color indices  $a, b$  and equal times  $x_0 = y_0$ , which transform under gauge transformations like [32,36]

$$O_{ab}^\Lambda(x, x_r) = \Lambda_{aa'}^\dagger(x) O_{a'b'}(x, x_r) \Lambda_{b'b}(x_r). \quad (22)$$

The simplest choice of such fields describing string-type states is  $U_{ab}(x, x_r)$  and for the meson-type states  $\Phi_a(x)\Phi_b^\dagger(x_r)$ . By  $U(x, y)$  we denote the product of gauge links along the straight line connecting  $y$  with  $x$ . The basic matrix correlation for the extraction of the static potentials can be expressed in terms of the following transition matrix elements [22]

$$C_{\text{WW}}(r, t) = \langle \text{tr} [U(x, x_r) U(x_r, x_r + t\hat{0}) U^\dagger(x + t\hat{0}, x_r + t\hat{0}) U^\dagger(x, x + t\hat{0})] \rangle, \quad (23)$$

$$C_{\text{WM}}(r, t) = \langle \Phi^\dagger(x + t\hat{0}) U^\dagger(x, x + t\hat{0}) U(x, x_r) U(x_r, x_r + t\hat{0}) \Phi(x_r + t\hat{0}) \rangle, \quad (24)$$

$$C_{\text{MM}}(r, t) = \langle \Phi^\dagger(x + t\hat{0}) U^\dagger(x, x + t\hat{0}) \Phi(x) \Phi^\dagger(x_r) U(x_r, x_r + t\hat{0}) \Phi(x_r + t\hat{0}) \rangle. \quad (25)$$

The static quark (anti-quark) is represented by a straight time-like Wilson line  $U^\dagger(x, x + t\hat{0})$  ( $U(x_r, x_r + t\hat{0})$ ). The matrix  $C$  is real, symmetric and positive. This simplest choice of the states does not however correspond to the physical picture that we have of the system.

The string-type states should reproduce the flux tube [37,38,39,40,41,42] of the gauge field binding the static quarks. Therefore, we smear the space-like links describing the string-type states using the APE smearing procedure of [43] with smearing strength set to the numerical value  $\epsilon = 1/4$ . In order to construct “physical” two-meson states, we determine the spectrum of the static-light mesons as described in Sect. 2. In the matrix correlation eq. (5) we use smeared Higgs fields  $O_i^{\text{M}}(x) = \Phi_2^{(n_i)}(x)$  defined with the smearing operator of eq. (11). The numbers  $n_i$  ( $i = 1, 2, \dots, N$ ) denote the smearing levels. The eigenvectors  $v_\alpha \in \mathbb{R}^N$  ( $\alpha = 0, 1, 2, \dots$ ), obtained by solving the generalised eigenvalue problem eq. (7) for large  $t$ , are the wave functions describing approximately

(because of the finite basis of fields and the finite time  $t$ ) the true eigenstates of the Hamiltonian. We define the fields

$$\Psi_\alpha(x) = \sum_{i=1}^N v_{\alpha,i} \Phi_2^{(n_i)}(x) \quad (\alpha = 0, 1, 2, \dots), \quad (26)$$

corresponding to the approximate one-meson eigenstates. The fields we choose to describe two-meson states are defined as

$$[\Psi_\alpha(x)]_a \cdot [\Psi_\beta^*(x_r)]_b, \quad \alpha, \beta = 0, 1, 2. \quad (27)$$

The values  $\alpha = 0, 1, 2$  refer to the ground, first and second excited one-meson state. The field basis in eq. (27) contains combinations with  $\alpha \neq \beta$  which are not symmetric under interchange of the positions  $x$  and  $x_r$  of the static charges. Because we expect the ground two-meson state to be symmetric, we project into the symmetric linear combinations of the fields in eq. (27) when we analyse the data of the simulations. The “mixed” states (for example of one meson in the ground state and one meson in the first excited state) can be important when looking at the asymptotic behavior (in  $r$ ) of excited static potentials [44]. The one-meson states have a space extension due to the smearing of the Higgs field. For a high number of smearing iterations, there is effectively an “interaction” between the mesons in the two-meson states eq. (27) due to the overlap of the smeared Higgs fields

Summarising, we use the basis of states  $|i\rangle$  described by the fields

$$[O_i(x, x_r)]_{ab} = \begin{cases} U_{ab}^{(m_i)}(x, x_r) & i = 1, 2, \dots, N_U \\ [\Psi_{\alpha_i}(x)]_a [\Psi_{\beta_i}^*(x_r)]_b & i = N_U + 1, \dots, N_U + 9 \end{cases} \quad (28)$$

where  $U^{(m_i)}(x, x_r)$  is the product of smeared gauge links (with smearing level  $m_i$ ) along the straight line connecting  $x_r$  with  $x$  and the pairs of indices ( $\alpha_i = 0, 1, 2; \beta_i = 0, 1, 2$ ) label the 9 combinations of two-meson states. We construct the following matrix correlation

$$C_{ij}(t, r) = \langle [O_i(x, x_r)]_{ab} U_{bc}(x_r, x_r + t\hat{0}) [O_j(x + t\hat{0}, x_r + t\hat{0})]_{cd}^\dagger U_{da}^\dagger(x, x + t\hat{0}) \rangle. \quad (29)$$

We denote the static potentials by  $V_\alpha(r)$ ,  $\alpha = 0, 1, 2, \dots$ . The corresponding eigenstates of the Hamiltonian are denoted by  $|\alpha\rangle$ . Taking the limit of infinite time extension of the lattice  $T \rightarrow \infty$ , we obtain from the transfer matrix formalism the following spectral representation of eq. (29) [32]

$$C_{ij}(t, r) = \sum_{\alpha} \langle j|\alpha\rangle \langle \alpha|i\rangle e^{-tV_\alpha(r)}. \quad (30)$$

For fixed separation  $r$ , we extract from  $C(t, r)$  the potentials  $V_\alpha(r)$  using the variational method described in Sect. 2.2.

fields	smearing levels $m$
$U^{(m)}$ (see [43] with $\epsilon = 1/4$ )	7,10,15
$\Phi_2^{(m)}$ (see eq. (11))	1,3,5,7,10,15

**Table 1:** Here, we list the smearing levels for the gauge and Higgs fields used in the simulation with parameters  $\beta = 2.4$ ,  $\kappa = 0.2759$ ,  $\lambda = 0.7$ .

### 3.2 Results at $\beta = 2.4$

In our first study [22] we obtained the static potential from a simulation at  $\beta = 2.2$ ,  $\kappa = 0.274$ ,  $\lambda = 0.5$  on a  $20^4$  lattice. We observed string breaking at a distance  $r_b/a \approx 5$ . We decided then to study the system with a better lattice resolution at  $\beta = 2.4$ . The results that we describe in the following are obtained on a  $32^4$  lattice for the parameter set

$$\beta = 2.4, \quad \kappa = 0.2759, \quad \lambda = 0.7. \quad (31)$$

The field basis is constructed according to eq. (26) and eq. (28) from smeared gauge ( $N_U = 3$ ) and Higgs fields, whose smearing parameters are summarised in Table 1. The parameters for the simulation were fixed after some trial runs. In the matrix correlation function  $C_{ij}(t, r)$  ( $i, j = 1, 2, \dots, 12$ ), the time-like links are replaced by their one-link integrals [35]. We collected a statistics of 800 measurements. Autocorrelations in the measurements are practically absent: the statistical errors, computed by a jackknife analysis remain constant when we group the measurements in bins of length 1,2 or 4.

#### 3.2.1 Renormalised static potentials

The static potentials  $V_\alpha(r)$  ( $\alpha = 0, 1, 2, \dots$ ) are extracted from the matrix correlation eq. (29) using the variational method described in Sect. 2.2. We rewrite eq. (9) as

$$aV_\alpha(r) = \ln(\lambda_\alpha(t - a, t_0)/\lambda_\alpha(t, t_0)) + \mathcal{O}\left(e^{-t\Delta V_\alpha(r)}\right), \quad (32)$$

where  $\Delta V_\alpha(r) = \min_{\beta \neq \alpha} |V_\alpha(r) - V_\beta(r)|$  and the eigenvalues  $\lambda_\alpha(t, t_0)$  are obtained by solving the generalised eigenvalue problem eq. (7) with the matrix correlation function at fixed  $r$ . We choose  $t_0 = 0$ . At all distances  $r$  we can read off with confidence and very good statistical precision (per mille level) values for the static potential  $V_0(r)$  at  $t = 7a$  which agree fully with  $t = 6a$ . From the static potential along a lattice axis we determined the scale  $r_0$  exactly as explained in [2]. The result is

$$r_0/a = 5.29(6). \quad (33)$$

Comparing this number with the values of  $r_0/a$  computed in quenched QCD [45], we see that our point eq. (31) in the SU(2) Higgs model corresponds in resolution to  $\beta \approx 6$

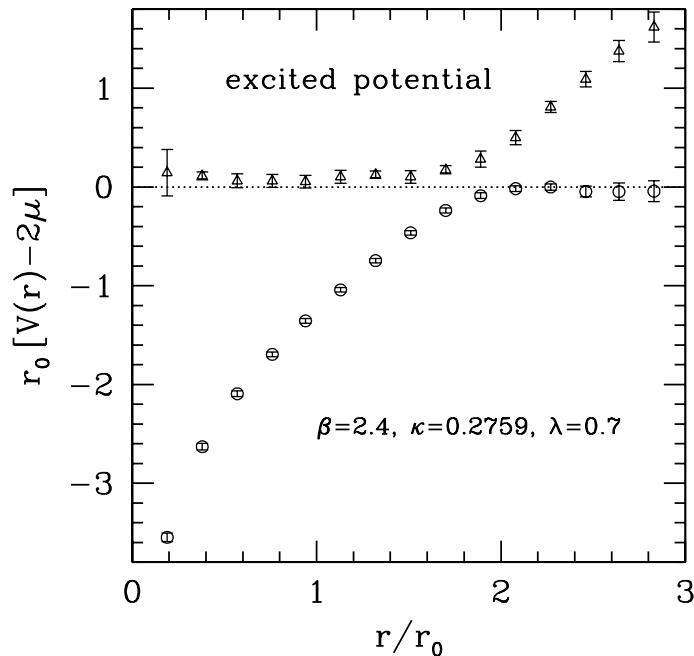


**Figure 5:** Here, the renormalised ground state and first excited state static potentials in units of  $r_0$  are shown as functions of the separation of the static quarks. String breaking is clearly visible at  $r_b \approx 1.9r_0$  together with the crossing of the energy levels.

in the SU(3) Yang-Mills theory with Wilson action. With respect to our first work [22], the lattice resolution is almost a factor 2 better.

The static potentials  $V_\alpha(r)$  as they are obtained from eq. (32) are not renormalised quantities because they contain self-energy contributions of the static quarks which diverge like  $1/a$  in the continuum. We consider instead the differences  $V_\alpha(r) - 2\mu$  which are free of divergences [32] and multiply them by  $r_0$  to obtain dimensionless renormalised potentials. In Fig. 5, we represent the ground state and the first excited state static potentials. The ground state potential shows an approximate linear rise at intermediate distances: around separation

$$r_b \approx 1.9 r_0 \quad (34)$$

the potential flattens: the string breaks. As expected, for large distances the potential approaches the asymptotic value  $2\mu$ . The first excited potential comes very close to the ground state potential around  $r_b$  and rises linearly at larger distances. The scenario of string breaking as a level crossing phenomenon [30] is confirmed beautifully.

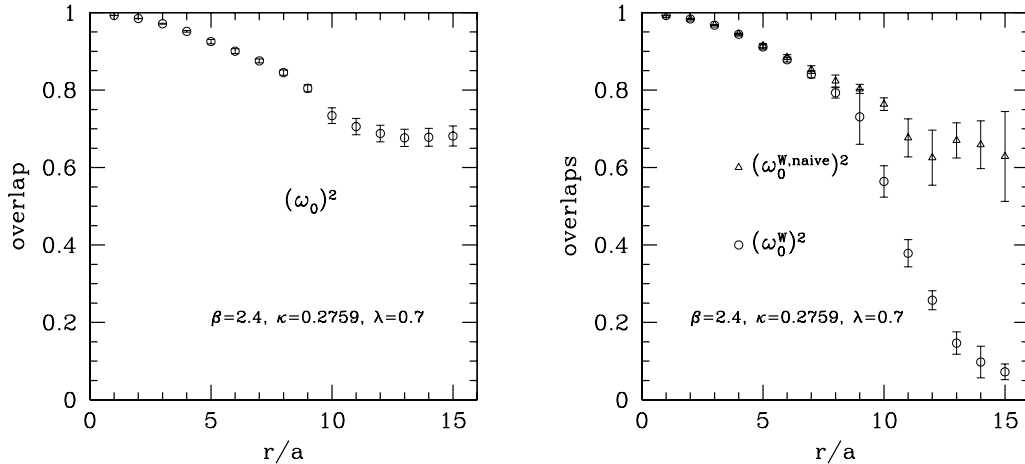


**Figure 6:** In the figure on the left, we show the overlap  $\omega_0$  obtained using the full basis of states eq. (28). In the figure on the right, we show the overlap  $\omega_0^W$  determined from string-type states only (described by the Wilson loops). A “naive” way of extracting it (triangles), using eq. (36), gives an erroneous large overlap at long distances. A safe estimate (circles) is obtained from eq. (37).

### 3.2.2 Overlaps

A certain measure for the efficiency of a basis of fields eq. (28) used to extract the ground state potential is given by the *overlap*. Using the approximate ground state wave function  $v_0$  obtained from the variational method we define the projected correlation function

$$\Omega(t) = \sum_{i,j} v_{0,i} C_{ij}(t) v_{0,j} = \sum_{\alpha} (\omega_{\alpha})^2 e^{-tV_{\alpha}(r)}, \quad (35)$$

with normalisation  $\Omega(t_0 = 0) = 1$ . The positive coefficients  $(\omega_{\alpha})^2$  may be interpreted as the square of the overlap of the true eigenstates of the Hamiltonian  $|\alpha\rangle$  with the approximate ground state characterized by  $v_0$ . The “overlap” is an abbreviation commonly used to denote the ground state overlap,  $\omega_0$ . We determine  $\omega_0$  straightforwardly from the correlation function  $\Omega(t)$  by noting that

$$\ln(\omega_0)^2 \underset{t \rightarrow \infty}{\sim} \frac{t+a}{a} \ln \Omega(t) - \frac{t}{a} \ln \Omega(t+a). \quad (36)$$

We extract safe values for  $(\omega_0)^2$  at  $t = 7a$ , which agree fully with  $t = 6a$  and are shown in the left part of Fig. 6. Our basis of fields is big (and good) enough such that  $(\omega_0)^2$  exceeds about 60% for all distances.

It is interesting to consider also the overlap for the (smeared) Wilson loops alone, i.e. we restrict the matrix correlation function to the  $3 \times 3$  sub-block associated with

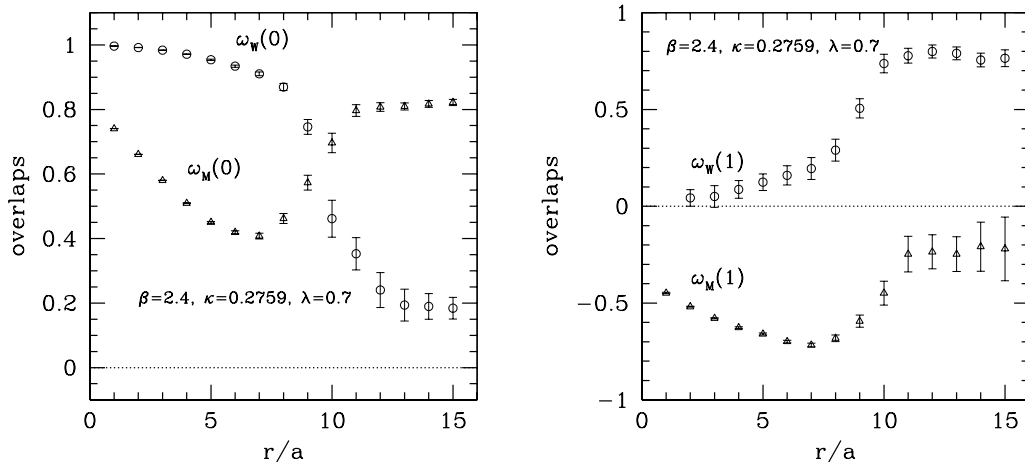


**Figure 7:** In the figure on the left, the overlaps of the string-type (circles) and meson-type (triangles) states with the ground state of the Hamiltonian are shown as functions of the separation  $r$  of the static quarks. In the figure on the right, the same overlaps but with the first excited eigenstate of the Hamiltonian are shown.

string-type states. Let us denote the corresponding projected correlation function by  $\Omega_W(t)$  and the overlap by  $\omega_0^W$ . The computation of  $\omega_0^W$  is more difficult because it turns out to be very small at large  $r$ . In the right part of Fig. 6, we present the results for two estimates of  $(\omega_0^W)^2$ . The triangles correspond to the estimates  $(\omega_0^{W,\text{naive}})^2$  obtained directly from eq. (36), with  $\Omega(t)$  replaced by  $\Omega_W(t)$ . The circles correspond to the more reliable estimate using the information from the full matrix correlation: the expression

$$(\omega_0^W)^2 \underset{t \rightarrow \infty}{\sim} (\omega_0)^2 \frac{\Omega_W(t)}{\Omega(t)} \quad (37)$$

converges reasonably fast and  $(\omega_0^W)^2$  can be estimated from the r.h.s. for large  $t$  ( $t/a = 7 - 9$  in practice). Using eq. (37), we see that (smeared) Wilson loops alone have an overlap which drops at intermediate distances and they are clearly inadequate to extract the ground state at large  $r$ . On the contrary,  $(\omega_0^{W,\text{naive}})^2$  is above 50% at large distances: what is estimated here, is actually the coefficient  $(\omega_1^W)^2$ , i.e. the square of the overlap of the (smeared) Wilson loops with the first excited state (this statement is supported by direct calculation, see Sect. 3.2.3). The fact that  $\omega_1^W$  is so large might explain the problems encountered in QCD for observing string breaking from the analysis of a correlation matrix with Wilson loops only.

### 3.2.3 Mixing

Finally, we want to show that string breaking is a mixing phenomenon involving string-type and meson-type states. This leads to the crossing of the energy levels seen above.



We consider the diagonal sub-blocks of the matrix correlation function eq. (29) corresponding to string-type states (fields  $i = 1, 2, 3$  in eq. (28)) and to meson-type states (fields  $i = 4, 5, \dots, 12$  in eq. (28)) separately. We determine approximate ground state wave functions  $v_0^{\text{W}}$  in the subspace of the string-type states and  $v_0^{\text{M}}$  in the subspace of the meson-type states. With the help of these wave functions we construct a  $2 \times 2$  projected matrix correlation function

$$\Omega_{kl}(t) = \sum_{i,j} v_{0,i}^k C_{ij}(t) v_{0,j}^l = \sum_{\alpha} \langle \psi_l | \alpha \rangle \langle \alpha | \psi_k \rangle e^{-tV_{\alpha}(r)} \quad (k, l = \text{W}, \text{M}), \quad (38)$$

where

$$|\psi_k\rangle = \sum_i v_{0,i}^k |i\rangle. \quad (39)$$

An inspection of

$$\Omega_{\text{WM}}(t_0 = 0) = \langle \psi_{\text{M}} | \psi_{\text{W}} \rangle \quad (40)$$

shows that string-type and meson-type states are orthogonal only for large values of  $r$  [32]. The coefficients

$$\omega_k(\alpha) \equiv \langle \alpha | \psi_k \rangle \quad (k = \text{W}, \text{M}), \quad (41)$$

in the expansion eq. (38), express the overlap of the string-type ( $k = \text{W}$ ) and meson-type ( $k = \text{M}$ ) states with the true eigenstates of the Hamiltonian. We can choose our phase conventions for the states such that the coefficients  $\omega_k(\alpha)$  are real and in addition  $\omega_{\text{W}}(0) > 0$  and  $\omega_{\text{W}}(1) > 0$ . We truncate the sum in eq. (38) after  $\alpha = 1$  and consider the diagonal matrix elements  $\Omega_{kk}(t)$  for two fixed times  $t = t_1$  and  $t = t_2$ : inserting the known values for  $V_0(r)$  and  $V_1(r)$ , we can solve for  $\omega_k^2(0)$  and  $\omega_k^2(1)$ . The sign of the coefficients  $\omega_{\text{M}}(0)$  and  $\omega_{\text{M}}(1)$  is fixed by the off-diagonal matrix elements  $\Omega_{\text{WM}}(t_1)$  and  $\Omega_{\text{WM}}(t_2)$ : we find that for all  $r$ ,  $\omega_{\text{M}}(0) > 0$  and  $\omega_{\text{M}}(1) < 0$  (in our sign convention). The overlaps  $\omega_{\text{W}}(0)$  of the string-type states (circles) and  $\omega_{\text{M}}(0)$  of the meson-type states (triangles) with the ground state of the Hamiltonian are shown on the left of Fig. 7 and the corresponding overlaps  $\omega_{\text{W}}(1)$  and  $\omega_{\text{M}}(1)$  with the first excited eigenstate of the Hamiltonian on the right of Fig. 7. String-type states have a large overlap at short distances with the ground state and at large distances with the first excited state. Meson-type states have a large overlap at short distances with the first excited state and at large distances with the ground state.

In addition, we observe that the overlap of the meson-type states with the ground state is also large at very short distances. The explanation for this fact is that string-type and meson-type states have an overlap with each other at short distances. In the string breaking region around  $r/a = 9 - 10$ , the overlaps of the string-type and meson-type states have similar magnitude, both when the ground state or the first excited state is considered. This fact is reflected in the crossing of the energy levels Fig. 5. Here, we

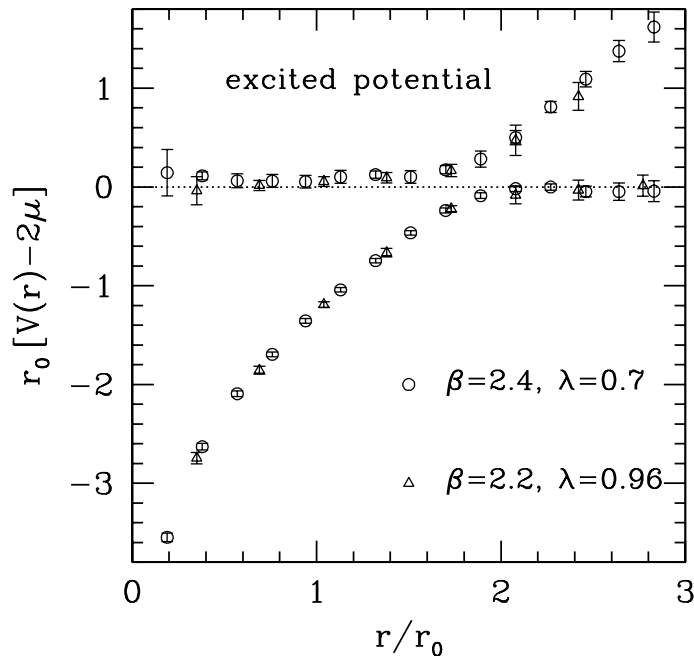


**Figure 8:** Here, we show the scaling of the renormalised ground state and first excited state static potentials. The parameter points lie on a line of constant physics.

would like to point out that the overlaps represented in Fig. 7 are not quantities which have a strict continuum limit. They depend on the  $\beta$ -value and the other parameters (e.g. of the smearing) that we consider. However, as long as one chooses a good basis (say with  $\omega_0 > 0.5$ ) which can be separated into “string like” and “meson like”, the qualitative behavior in Fig. 7 is expected to persist also at smaller lattice spacings.

#### 4 Scaling of the static potentials

In order to compare the renormalised static potentials at different values of the lattice spacing and estimate the size of scaling violations, a way of determining *lines of constant physics* (LCP) in the confinement “phase” of the SU(2) Higgs model is needed. This question has been addressed in [31], where a non-perturbative determination of the LCPs is described.

The bare parameters  $\kappa$  and  $\lambda$  are renormalised along a LCP by keeping two physical quantities  $F_1$  and  $F_2$  constant. A good choice is to take

$$F_1 = r_0 [2\mu - V_0(r_0)] \quad (42)$$

and  $F_2$  to be the generalised Binder cumulant  $c_3$  defined in [31].<sup>7</sup>

<sup>7</sup> Physically  $F_1$  is a (non-perturbative) measure of the Higgs mass: the variation of  $F_1$  with the

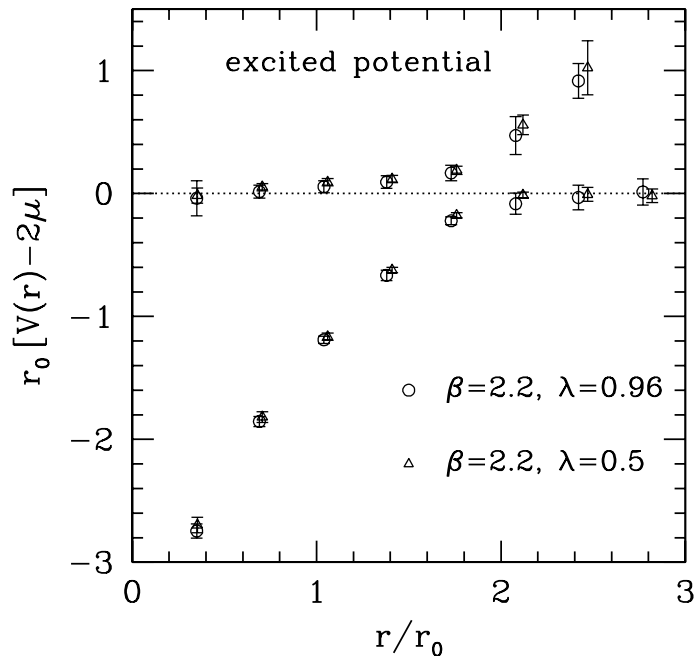


**Figure 9:** Here, we show the  $\lambda$ -independence of the static potentials. The parameter  $\kappa$  is determined from eq. (45).

Taking the parameter set (31) which we used in the simulation at  $\beta = 2.4$  we obtain the conditions

$$F_1 = F_1^* \equiv 1.26 \quad \text{and} \quad F_2 = F_2^* \quad (43)$$

defining a LCP (the numerical value  $F_2^*$  can be found in [31]). As a result of the non-perturbative matching, the parameter sets (31) and

$$\beta = 2.2, \quad \kappa^* = \kappa(\lambda^*), \quad \lambda^* = 0.96(10) \quad (44)$$

lie on a LCP. The value of  $\kappa$  at  $\beta = 2.2$  is determined using the polynomial fit [31]

$$\begin{aligned} \kappa(\lambda) = & 0.3131 + 0.0564(\lambda - 1) - 0.0286(\lambda - 1)^2 \\ & + 0.0198(\lambda - 1)^3 - 0.0246(\lambda - 1)^4 \end{aligned} \quad (45)$$

which is obtained by requiring  $F_1 = F_1^* \equiv 1.26$  and correlates the uncertainties in  $\kappa$  and  $\lambda$  of the LCP. In Fig. 8, we compare the results for the renormalised ground state and bare parameters is dominantly caused by the variation of the meson mass  $\mu$ . This bound state mass is of course expected to depend strongly on the mass of its constituents. On the other hand, the interpretation of  $F_2$  is less obvious. It was chosen to have a second renormalised quantity which is both sensitive to the bare coupling  $\lambda$  and can be computed in the MC simulations[31].

first excited state static potentials that we obtain at  $\beta = 2.4$  and at  $\beta = 2.2$  along the LCP. The results for the potentials are compatible with scaling within minute errors under variation of the lattice spacing by almost a factor 2.

Another interesting issue is the  $\lambda$ -dependence of physical observables. Exploratory results [46] indicated that the physics of the SU(2) Higgs model in the confinement “phase” is weakly dependent on  $\lambda$ . This is certainly true near the continuum limit because it is well accepted that the scalar part of the SU(2) Higgs model is a trivial theory. Nevertheless, at finite value of the lattice spacing the model can be considered as an *effective* field theory with three independent renormalised couplings. In Fig. 9, we compare the static potentials for two different values  $\lambda = 0.5$  and  $\lambda = 0.96$  at  $\beta = 2.2$ . The parameter  $\kappa$  is determined from eq. (45). There is no significant difference between the different  $\lambda$  values. This also means that the uncertainty in  $\lambda^*$  in (44) is irrelevant for our scaling test Fig. 8.

## 5 Conclusions

We presented the results for the static potentials (ground state and first excited state) in the confinement “phase” of the SU(2) Higgs model. The string breaking or flattening of the ground state potential is clearly visible around separation  $r_b \approx 1.9r_0$ . The comparison with the first excited potential shows a nice crossing of the energy levels. The interpretation of string breaking as level crossing phenomenon between string-type and meson-type states is substantiated by the investigation of properly defined overlaps.

We also addressed the question of scaling violations in the measurements of the static potentials. They are shown to be tiny already at  $r_0/a > 2.5$ . Moreover, the dependence of the static potentials on the Higgs quartic coupling  $\lambda$  is very weak once the parameter  $\kappa$  is determined by keeping the physical quantity  $F_1$  constant. These results are a strong indication for a continuum-like behavior of the static potentials already at the relatively large values of the lattice spacing that we used.

The method for the determination of the static potential that we presented can be applied in QCD. Some steps in this direction have already been made[28]. The main problem for QCD is the statistical accuracy.

**Acknowledgement.** We thank the Konrad-Zuse-Zentrum für Informationstechnik Berlin (ZIB) for granting CPU-resources to this project.

## References

- [1] UKQCD, S.P. Booth et al., Nucl. Phys. B394 (1993) 509, hep-lat/9209007.
- [2] R. Sommer, Nucl. Phys. B411 (1994) 839, hep-lat/9310022.
- [3] G.S. Bali and K. Schilling, Phys. Rev. D46 (1992) 2636.
- [4] UKQCD, S.P. Booth et al., Phys. Lett. B294 (1992) 385, hep-lat/9209008.

- [5] SESAM, U. Glässner et al., Phys. Lett. B383 (1996) 98, hep-lat/9604014.
- [6] S. Güsken, Nucl. Phys. Proc. Suppl. 63 (1998) 16, hep-lat/9710075.
- [7] UKQCD, C.R. Allton et al., Phys. Rev. D60 (1999) 034507, hep-lat/9808016.
- [8] CP-PACS, R. Burkhalter et al., Nucl. Phys. Proc. Suppl. 73 (1999) 3, hep-lat/9810043.
- [9] CP-PACS-Collaboration, S. Aoki et al., Phys. Rev. D60 (1999) 114508, hep-lat/9902018.
- [10] For a review see K. Schilling, to appear in the proceedings of the 17th International Symposium on Lattice Field Theory (Pisa 1999), Nucl. Phys. B Proc. Suppl. , hep-lat/9909152.
- [11] B. Bolder et al., (2000), hep-lat/0005018.
- [12] C. Alexandrou, S. Güsken, F. Jegerlehner, K. Schilling and R. Sommer, Nucl. Phys. B414 (1994) 815, hep-lat/9211042.
- [13] R. Sommer, Phys. Rept. 275 (1996) 1, hep-lat/9401037.
- [14] H. Joos and I. Montvay, Nucl. Phys. B225 (1983) 565.
- [15] P. Becher, Ann. Phys. 146 (1983) 223.
- [16] J. Potvin, Phys. Rev. D32 (1985) 2070.
- [17] H. Dilger, Phys. Lett. B294 (1992) 263.
- [18] J. Heitger, *Numerical Simulations of Gauge-Higgs Models on the Lattice*, PhD thesis at University of Münster (1997).
- [19] H.G. Evertz et al., Phys. Lett. 175B (1986) 335.
- [20] W. Bock et al., Z. Phys. C45 (1990) 597.
- [21] C. Michael, Nucl. Phys. Proc. Suppl. 26 (1992) 417.
- [22] ALPHA-Collaboration, F. Knechtli and R. Sommer, Phys. Lett. B440 (1998) 345, erratum: Phys. Lett. B454 (1999) 399, hep-lat/9807022.
- [23] O. Philipsen and H. Wittig, Phys. Rev. Lett. 81 (1998) 4056, hep-lat/9807020.
- [24] P.W. Stephenson, Nucl. Phys. B550 (1999) 427, hep-lat/9902002.
- [25] O. Philipsen and H. Wittig, Phys. Lett. B451 (1999) 146, hep-lat/9902003.
- [26] P. de Forcrand and O. Philipsen, Phys. Lett. B475 (2000) 280, hep-lat/9912050.

- [27] C. DeTar, O. Kaczmarek, F. Karsch and E. Laermann, Phys. Rev. D59 (1999) 031501, hep-lat/9808028.
- [28] UKQCD, P. Pennanen and C. Michael, (2000), hep-lat/0001015.
- [29] UKQCD, C. Michael and J. Peisa, Phys. Rev. D58 (1998) 034506, hep-lat/9802015.
- [30] I.T. Drummond, Phys. Lett. B434 (1998) 92, hep-lat/9805012.
- [31] ALPHA, F. Knechtli, Phys. Lett. B478 (2000) 387, hep-lat/9912031.
- [32] F. Knechtli, PhD thesis at Humboldt-University Berlin (1999), hep-lat/9910044.
- [33] M. Lüscher, Commun. Math. Phys. 54 (1977) 283.
- [34] M. Lüscher and U. Wolff, Nucl. Phys. B339 (1990) 222.
- [35] G. Parisi, R. Petronzio and F. Rapuano, Phys. Lett. 128B (1983) 418.
- [36] R. Sommer, *Static Potential and Chromo Field Strength Distribution in Lattice QCD*, PhD thesis at University of Wuppertal (1986).
- [37] G.S. Bali, K. Schilling and C. Schlichter, Phys. Rev. D51 (1995) 5165, hep-lat/9409005.
- [38] M. Lüscher, G. Münster and P. Weisz, Nucl. Phys. B180 (1981) 1.
- [39] R. Sommer, Nucl. Phys. B291 (1987) 673.
- [40] J. Wosiek and R.W. Haymaker, Phys. Rev. D36 (1987) 3297.
- [41] M. Caselle, F. Gliozzi, U. Magnea and S. Vinti, Nucl. Phys. B460 (1996) 397, hep-lat/9510019.
- [42] P. Pennanen, A.M. Green and C. Michael, Phys. Rev. D56 (1997) 3903, hep-lat/9705033.
- [43] APE, M. Albanese et al., Phys. Lett. 192B (1987) 163.
- [44] We thank F. Niedermayer for emphasising this point .
- [45] ALPHA, M. Guagnelli, R. Sommer and H. Wittig, Nucl. Phys. B535 (1998) 389, hep-lat/9806005.
- [46] I. Montvay, Nucl. Phys. B269 (1986) 170.